In and Si adatoms on Si(111)5×2-Au: Scanning tunneling microscopy and first-principles density functional calculations

A. Stępniak, P. Nita, M. Krawiec,* and M. Jałochowski
Institute of Physics, M. Curie-Skłodowska University, Pl. M. Curie-Skłodowskiej 1, 20-031 Lublin, Poland
(Received 24 June 2009; revised manuscript received 31 August 2009; published 30 September 2009)

Structural properties of monatomic indium chains on Si(111)5×2-Au surface are investigated by scanning tunneling microscopy (STM) and first-principles density functional calculations (DFT). The STM topography data show that submonolayer coverage of indium leads to a well-ordered chain structure with the same periodicity as the Si adatoms form on Si(111)5×2-Au surface. Bias-dependent STM topography and spectroscopy reveal two different mechanisms of In-atoms adsorption on the surface: bonding to Si adatoms and substitution for Si atoms in the adatom positions. Those mechanisms are further corroborated by DFT calculations. The obtained structural model of In-modified Si(111)5×2-Au surface remains in good agreement with the experimental data.

DOI: 10.1103/PhysRevB.80.125430 PACS number(s): 73.20.At, 71.15.Mb, 79.60.Jv, 68.35.B−

I. INTRODUCTION

Among various structural phases of Au-induced Si(111) surface,[1,2] the 5×2 reconstruction has become fascinating due to spontaneous formation of arrays of monatomic chains. The unit cell of this reconstruction is 1.625 nm ($5\times a_{[11\bar{2}]}$) wide and 0.768 nm ($2\times a_{[1\bar{1}0]}$) long, and is observed at the gold coverage 0.44 ML.[3] Since its discovery, the 5×2 reconstruction has been extensively investigated by number of experimental techniques, including low-energy electron diffraction,[1,2,4] x-ray diffraction,[5,6] high-resolution electron microscopy,[7] scanning tunneling microscopy (STM),[8–15] angle-resolved photoemission (ARPES),[14,16–20] and inverse photoemission.[21]

Parallel to experimental effort, theoretical investigations have been carried out in order to find a structural model of 5×2 reconstruction.[22–26] However, first attempts to the structural model utilized STM and diffraction experiments.[3,5,6,27] Two most complete structural models have been proposed by Marks and Plass based on a high-resolution transmission electron-diffraction data[7] and by Hasegawa, Hosaka, and Hosoki, deduced from STM experiments.[10] Both models have been examined by first-principles density functions calculations (DFT), and they turned out to fail to reproduce the key features of angle-resolved photoemission spectroscopy and STM topography data.[22,24] Later, Erwin[23] proposed another structural model of 5×2 reconstruction, deduced from DFT calculations, which has widely been used while interpreting STM topography data. This model features the presence of honeycomb chain,[28,29] which is a common feature of many Si surfaces.[30] Erwin's model well reproduces a number of STM observed features such as V-shaped and U-shaped features and less accurately bright protrusions (BP),[13] which are known to be Si adatoms.[11,12,14,20] Other theoretical models[24,26] having lower surface energies with respect to the Erwin's model suffer from similar problems as the Erwin's model does, namely, they do not reproduce reasonably well the Si adatoms in STM topography. Interestingly, the electronic band structure calculated within those models remain in good agreement with the ARPES data. Among the 5×2 structural models, the model proposed by Ren *et al.*[25] seems, at present, to be best candidate for structural model of 5×2 reconstruction, as it well describes the main features of STM topography together with the Si adatoms. Note that this model is based on the structure investigated in Ref. 24 and has the surface energy comparable to the Erwin model.

As it was already mentioned, characteristic feature of Si(111)5×2-Au surface is the presence of Si adatoms, which are observed in STM topography images as bright protrusions. Those adatoms form a 5×4 superlattice but only half of the superlattice sites are occupied by Si adatoms.[20] This equilibrium coverage for 5×4 superstructure manifests itself in 5×4 chains and empty segments in between. Those Si-adatom chains are responsible for a long-standing puzzle regarding metallic or insulating character of the ARPES spectra.[14,16–20] It turns out that at the Si-adatom coverage less than equilibrium one, the system shows metallic character while at higher coverages, it goes into insulating phase. This was recently confirmed in beautiful experiment by Choi *et al.*,[14] where the Si-adatom coverage was controlled in systematic way.

Naturally a question arises if other materials, in particular, metals, will also form some superstructures on Si(111)5×2-Au surface. The metallic materials would shed some light on different aspects of one-dimensional (1D) metals. We have chosen indium, as In atoms are known to form 1D structures on flat Si(111)7×7 surface,[31,32] as well as on vicinal Si surfaces.[33–35] Perhaps the best known example of 1D structure is 4×1 reconstruction (see Ref. 36 and references therein), where indium atoms deposited on flat Si surface self-assemble into a double zigzag chain structure. This system undergoes a metal-insulator transition (presumably of the Peierls type) at temperature around 120 K. On the other hand, In deposited on vicinal Si surfaces forms regular arrays of 1D chains, located at the step edge.[35] Thus it is interesting to study indium atoms on Si(111)5×2-Au reconstruction, displaying 1D ordering but on flat surface.

The purpose of the present work is to investigate In-induced reconstruction on Si(111)5×2-Au surface in submonolayer coverage of indium and see if In atoms at very low coverage will form similar superstructure as the Si adatoms do.

Using scanning tunneling microscopy and spectroscopy we study structural properties of In chains on Si(111)5 $\times$2-Au surface. Our STM topography data show that, indeed, a submonolayer coverage of In leads to a well-ordered chain structure with the same periodicity as the Si adatoms form on 5×2 reconstruction. Moreover, the bias-dependent STM topography and spectroscopy reveal two different mechanisms of In adsorption on the surface. Namely, the bonding of In atoms to Si adatoms and adsorption in unoccupied Si-adatom positions. The DFT calculations show that both mechanisms are energetically almost degenerate. We propose structural model of In-modified Si(111)5×2-Au surface, derived from total-energy DFT calculations, which remains in good agreement with experimental data. The rest of the paper is organized as follows. In Secs. II and III details of experiment and of calculations are presented. Structural properties of clean and In-modified Si(111)5×2-Au surface are discussed in Secs. IV and V, respectively, while the electronic properties are presented in Sec. VI. We end up with conclusions in Sec. VII.

II. EXPERIMENTS

Experiments have been carried out in ultrahigh vacuum chamber with base pressure less then 5×10^{-11} mbar. The chamber was equipped with scanning tunneling microscope (type OmicronVT) and reflection high-energy electron-diffraction (RHEED) apparatus. The substrate used in the experiment was cut from a B-doped mirror-polished Si(111) wafer with a resistivity of 0.13 Ω cm. The Si(111) substrate was cleaned by flash anneal process up to 1500 K. The Si(111)5×2-Au surface was obtained by deposition of 0.5 ML of Au [in units of half of Si(111) double layer], heating the sample at temperature 1100 K for 20 s and gradually cooling down to the room temperature (RT) for 3 min. The quality of the surface has been controlled by RHEED technique. During the deposition of gold the Si sample was held at the room temperature. Next, submonolayer coverage (0.025 ML) of In was deposited onto the surface and then the sample was annealed at approximately 750 K for 1 min. The STM measurements were performed at temperature 100 K. Although STM imaging was performed at RT as well, essentially no difference was found between 100 K and the RT results, besides better resolution and less thermal drift due to enhanced stability at low temperature.

III. DETAILS OF CALCULATIONS

The calculations have been done using the SIESTA code, which performs standard pseudopotential density functional calculations in a basis of numerical atomic orbitals.[37–41] The local-density approximation[42] and Troullier-Martins norm-conserving pseudopotentials[43] have been used in calculations. The pseudopotentials of Au- and In-contained semicore states $5d$ and $4d$, respectively. A double-ζ polarized basis set was used for all the atomic species.[38,39] The radii of the orbitals for different species were following (in a.u.): Si-7.96($3s$), 7.98($3p$), and 4.49($3d$), Au-7.20($5d$), 6.50($6s$), and 5.85($6p$), In-3.43($4d$), 5.80($5s$), 7.83($5p$), and 6.57($5d$), and H-7.55($1s$) and 2.94($2p$). Due to large real-space supercell, only four nonequivalent k points for Brillouin-zone sampling and a real-space grid equivalent to a plane-wave cutoff 100 Ry were employed.

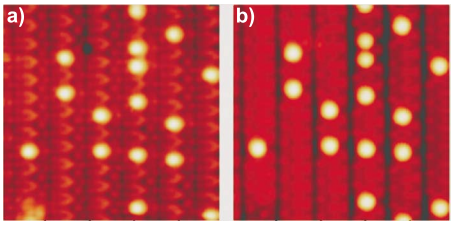

FIG. 1. (Color online) STM topography of the same area (10×10 nm^2) of Si(111)5×2-Au surface at $T=100$ K, recorded at tunneling current $I=0.37$ nA and bias voltages: (a) $U=+1.2$ V and (b) $U=-0.8$ V. The Si adatoms are visible as bright protrusions.

The Si(111)5×2-Au and Si(111)5×2-Au/In systems have been modeled by four silicon double layers and a vacuum region of 14 Å. All the atomic positions were relaxed until the maximum force was less than 0.04 eV/Å, except the Si atoms in the bottom layer, which were fixed at their bulk ideal positions and saturated with hydrogen. The lattice constant of Si was fixed at the calculated value, 5.39 Å.

IV. Si(111)5×2-Au SUBSTRATE

Figure 1 shows STM topography of an (a) empty- and a (b) filled-state images of the same area (10×10 nm^2) of the Si(111)5×2-Au surface. Some characteristic features can be observed. The empty-state STM topography image [panel (a)] shows so-called V-shaped protrusion (leg) between two balls (heads) in each unit cell.[8,13] Although it is known as second kind of the unit cell of 5×2 reconstruction composed of U-shaped protrusion under the head,[13] it is not observed in the present experiment. The bright protrusions, which are known to be Si adatoms, are observed at both voltage polarizations. It is known that the Si adatoms have a tendency to form a superstructure along $[1\bar{1}0]$ direction with a periodicity of $4\times a_{[1\bar{1}0]}$ but only half of the superlattice sites are occupied by Si adatoms.[20,44] Our experiment confirms such a behavior, although the distance $2\times a_{[1\bar{1}0]}$ between Si adatoms has also been observed accidentally.

Usually, while interpreting STM topography images one uses the structural model proposed by Erwin.[23] Although this model shows rather good agreement with main experimentally observed features, there is a discrepancy regarding Si adatoms. Namely, the calculated positions of the Si adatoms do not coincide with those observed in experiment. This is clearly visible in Fig. 2, where the comparison of the Erwin model with our (a) empty- and (b) filled-state STM topography images is shown.

The positions of the Si adatoms, calculated within this model are marked with small dark circles. Clearly, the calculations give wrong positions of the adatoms. While in experiment the Si adatoms are localized on the symmetry axis of the V-shape features, in calculations they are located out-

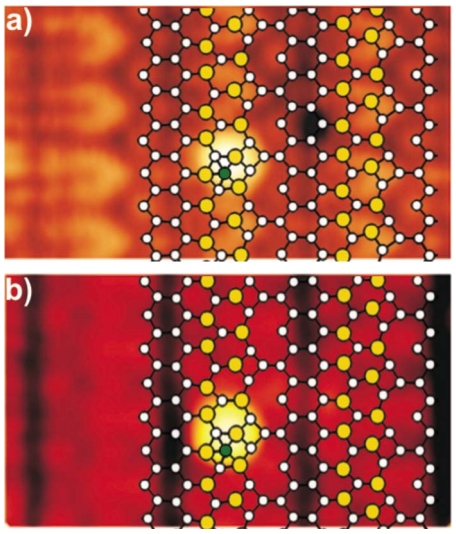

FIG. 2. (Color online) STM topography images (5.6 ×2.7 nm^2) of the same area of Si(111)5×2-Au surface, recorded at sample biases (a) U=+1.2 V and (b) U=−0.8 V. Light large (orange) and small white circles represent the Au and Si atoms, respectively, while small dark (green) circle is for Si adatom, deduced from the Erwin model (Ref. 23).

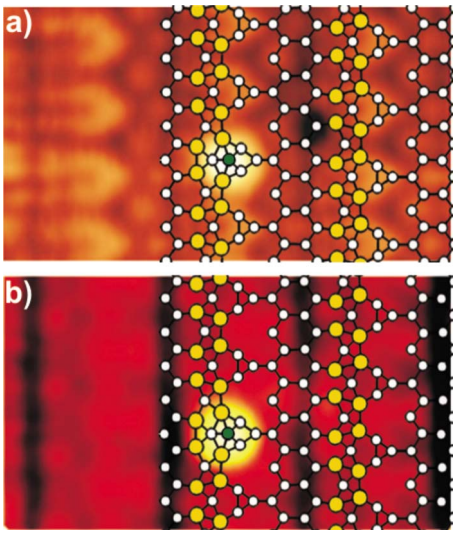

FIG. 3. (Color online) Comparison of structural model proposed by Ren *et al.* (Ref. 25) with the same STM topography data as in Fig. 2. Light large (orange) and small white circles represent the Au and Si atoms, respectively, while small dark (green) circle marks the Si adatom in this model.

side the V shapes. Similar behavior has been observed by Yoon *et al.*[13]

Recently another structural model of 5×2 reconstruction has been proposed by Ren *et al.*[25] This model is based on the structure investigated in Ref. 24 and has the surface energy comparable to the Erwin's model. This model also accounts for most of the features visible in STM topography data. What is more important, it also gives correct positions of the Si adatoms. Therefore we use the Ren's model to interpret the experimental data, rather than the Erwin's one. A comparison of our STM data with the structural model proposed by Ren[25] is shown in Fig. 3. Clearly, this model shows better agreement with the experimental data. In particular, the calculated positions of Si adatoms now coincide with the bright protrusions visible in STM topography.

V. Si(111)5×2-Au SURFACE MODIFIED BY In ADSORPTION

As it was previously mentioned, the Si adatoms form their own 5×4 superstructure with partial occupancy. It would be interesting to see if indium atoms will form similar superstructure. Therefore we deposited on Si(111)5×2-Au surface 0.025 ML of In atoms, which gives exactly one In atom per 5×8 unit cell. Figure 4 shows STM topography images of the 5×2 surface covered with 0.025 ML of In. Depending on the sample bias the different STM topography is observed. While at positive sample bias [panel (a)] several bright protrusions are observed, at negative bias [panel (b)] only some of them are visible. Moreover, at positive polarization a characteristic features of 5×2 reconstructions, namely, the V shapes, are observed. Comparing the images taken at different sample polarizations we could expect that the bright protrusions observed at positive polarization only (BP1) are the indium atoms while those observed at both polarizations (BP2) are the Si adatoms. Such a picture could be supported by following argument. The positions of BP2 on In-covered Si(111)5×2-Au surface coincide with the positions of Si adatoms on bare Si(111)5×2-Au surface. However, scanning tunneling spectroscopy (STS) spectra as well as DFT calculations show that the situation is more complicated. Namely, the bright protrusions observed in empty-state STM topography (BP1) are the In atoms bonded to Si adatoms while the bright protrusions observed at both polarizations are the Si adatoms (BP) and the In atoms located in positions expected for Si adatoms (BP2). Similar mechanisms of In adsorption have been observed in STM study of Si(111)7×7 surface.[44,45] Those include (i) In-atoms adsorption on top of the Si adatoms—BP visible at both polarizations, (ii) substitution of In for Si atoms in 7×7 adatom position—BP observed in empty-state images, and (iii) charge redistribution from Si rest atoms to nearby Si adatoms caused by In adsorption on the Si rest atoms—BP visible in

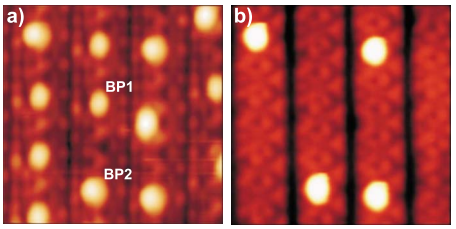

FIG. 4. (Color online) STM topography of the same area (6 ×6 nm^2) of Si(111)5×2-Au surface covered with 0.025 ML of In. Bias voltage is (a) U=+1.4 V and (b) U=−1.4 V, and the tunneling current is 0.2 nA. BP1 stands for one of bright protrusions composed of In atoms bonded to Si adatoms while BP2 marks one of the bright protrusions associated with In atoms located in Si-adatom positions.

the filled-state images. Those mechanisms have been deduced from bias-dependent STM topography images. In the case of Si(111)5×2-Au surface, our STM/STS and DFT investigations show that those mechanisms lead to different behavior of bright protrusions in bias-dependent STM topography, then it was proposed for 7×7 reconstruction. Namely, the protrusions observed at both polarizations are the In atoms located in 5×2 adatom position [mechanism (ii)]. The BP visible only in empty-state STM images are the In atoms bonded to Si adatoms, and both, (i) and (iii) processes are involved in this case. To be more precise, In atoms form covalent bonds with Si adatoms and rest atoms which lead to charge redistribution. However, unlike on Si(111)7×7 surface, the charge transfer takes place mainly from In atoms to Si adatoms and to underneath Si atoms, and very weak charge transfer from Si rest atoms. Such different behavior of BP on Si(111)5×2-Au and Si(111)7×7 surfaces may have its origin in different surface morphology, as the 5×2 reconstruction contains Au atoms.

Figure 5 shows two structural models of In-induced Si(111)5×2-Au reconstruction derived from DFT calculations. Panel (a) shows a side view and top view of a model with In atoms bonded to Si adatoms (model "bonded"), and panel (b) shows a model with In atoms substituted for Si atoms in adatom positions (model "substituted"). In model bonded, shown in panel (a), the In atoms are shifted in $[\bar{1}10]$ direction with respect to Si adatoms. However, they can also be shifted in opposite, i.e., in $[1\bar{1}0]$ direction (not shown), which is also observed in STM. Both positions are energetically degenerate. The bonding of In atoms to Si adatoms results in shifting of the positions of Si adatoms. The lateral positions of Si adatoms change by 0.1 Å while vertical ones by 0.2 Å. The Si adatoms are pushed toward the surface while In atoms stick out by 1.5 Å. In model substituted the lateral positions of the In atoms remain more or less the same as the positions of original Si adatoms. The only change is in vertical position by 0.9 Å out of the surface.

Both models are almost energetically degenerate, with model substituted having lower surface energy by ~0.3 meV/Å^2 only. Thus, on the basis of calculations, we cannot indicate which mechanism of adsorption is favorable. However, our STM data, show that mechanism (i), i.e., bonding to Si adatoms, is more preferred. On bare Si(111)5×2-Au surface, the number of BP (Si adatoms) is equal to one Si adatom per 5×8 unit cell. Although Si adatoms are known to form chains with ×4 periodicity, half of the adatom sites is occupied, thus equilibrium coverage is one Si adatom per 5×8 unit cell. In fact, number of BP strongly depends on sample preparation conditions,[14,20] and in our experiment, the Si-adatom occupancy is around 53%. All the BP are visible at both polarizations. When 0.012 ML of In (1 In atom per 5×16 unit cell) is deposited, the occupancy of Si-adatom 5×4 sites increases to 58%. At this In coverage all three kinds of bright protrusions, namely, BP1, BP2, and BP, are observed. BP1 amount to 40% of total number of protrusions while BP2 to 3% only. The remained 57% are Si adatoms (BP). When In coverage is further increased to 0.025 ML of In (1 In atom per 5×8 unit cell), the occupancy of Si-adatom 5×4 sites increases to 75%. Number of bright protrusions visible at positive bias, i.e., BP1 is equal 59% of all protrusions present and 8% of total number of protrusions are In atoms located in Si-adatom sites while remained 33% are the Si adatoms alone. The above data are summarized in Table I and clearly indicate that mechanism (i) is more favorable.

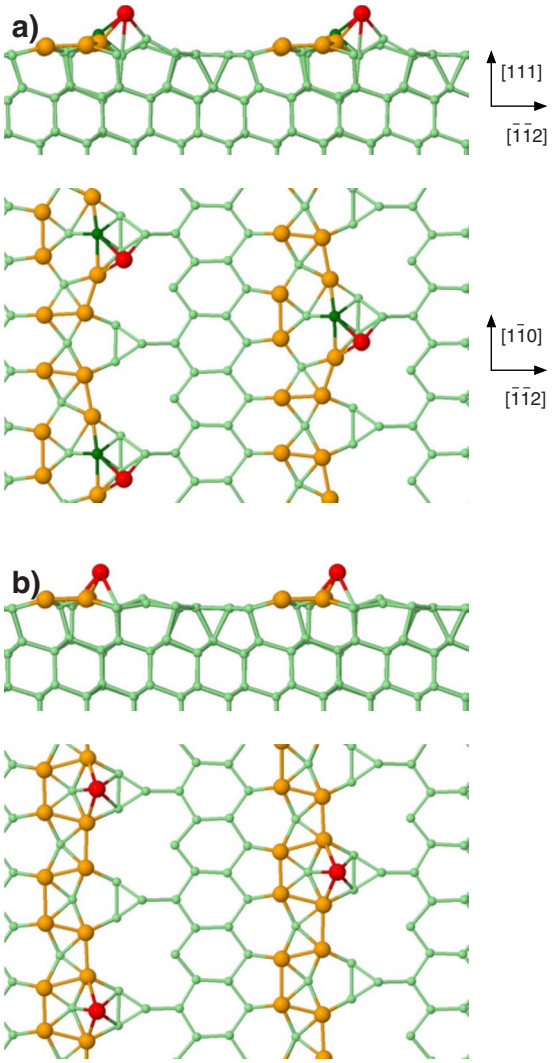

FIG. 5. (Color online) Structural models of In-covered Si(111)5×2-Au surface reflecting two different kinds of In adsorption. Panel (a) shows side view and top view of a model with In atoms bonded to Si adatoms (model "bonded") and panel (b) shows a model with In atoms substituted for Si atoms in adatom positions (model "substituted"). Different colors reflect different species of the structure: Si atoms—small light green circles, Au—large orange circles, In—large red circles, and Si adatoms—small green circles. Crystallographic directions are also indicated in panel (a).

As a result, one observes 1D chain structure composed of three kinds of protrusions, i.e., In atoms adsorbed on Si-adatom sites, In atoms bonded to Si adatoms and Si adatoms. The distance between the bright protrusions of any kind within the chain is equal to 1.54 nm, i.e., $4\times a_{[1\bar{1}0]}$. This distance is characteristic for Si(111)5×2-Au surface.[14] Similar as on Si(111)5×2-Au surface, characteristic features, i.e., the V shapes located between BP are also observable (see Fig. 4).

TABLE I. Occupancy of allowed Si(111)5×2-Au sites by bright protrusions (BP_{tot}) and contribution of different kinds of bright protrusions (BP, BP1, and BP2) to BP_{tot} vs In coverage.

In coverage [ML]	0.000	0.012	0.025
BP_{tot} [%]	53	58	75
BP/BP_{tot} [%]	100	57	33
$BP1/BP_{tot}$ [%]	0	40	59
$BP2/BP_{tot}$ [%]	0	3	8

A comparison of the STM topography of In-covered Si(111)5×2-Au surface together with both our models (Fig. 5) is shown in Fig. 6. Clearly, one observes very good agreement between STM data and the proposed structural models. In particular, the model bonded, gives asymmetrical positions of In atoms with respect to other characteristic features of 5×2 reconstruction.

The asymmetry in arrangement of BP1 within the 5×4 unit cell is presented in Fig. 7, where the line profiles across [panel (b)] and along [panel (c)] the chain shown in panel (a) are presented. This asymmetry is visible in the shift of BP1 with respect to neighboring atoms in $[1\bar{1}0]$ direction [compare profiles C and D in panel (b)]. The value of the shift is estimated to be 0.1 nm. As one can read off from panel (a), the protrusion BP2 is not shifted. This asymmetry in positions of BP1 modifies also local charge distribution on neighboring atoms, indicated by black arrows in panel (a). At higher In coverage the asymmetry is even more pronounced, in particular, at negative bias, where the shifts of In atoms are observed in both directions along the chain. Furthermore, the BP1 are shifted in $[\bar{1}\bar{1}2]$ direction with respect to original

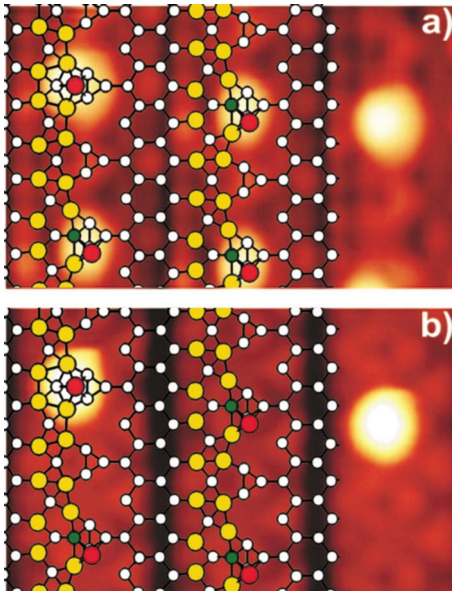

FIG. 6. (Color online) STM images (4.2×2.7 nm^2) of (a) empty state (+1.4 V) and (b) filled state (−1.4 V) of the same area. Light large (orange), small white, large dark (red), and small dark (green) circles represent the Au, Si, In atoms, and Si adatoms, respectively.

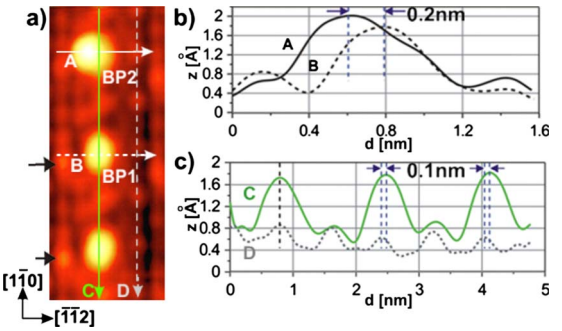

FIG. 7. (Color online) Panel (a) shows STM image (2×5 nm^2) of In-covered Si(111)5×2-Au surface; (b) profile lines across one of the chains (in $[\bar{1}\bar{1}2]$ direction), indicated in panel (a) as A and B. Panel (c) shows profile lines C and D along the chain (in $[1\bar{1}0]$ direction).

Si adatoms on Si(111)5×2-Au surface by 0.2 nm [see Fig. 7(b)].

In case of bare Si(111)5×2-Au surface, the presence of Si adatoms influences the STM topography of V-shape features. Namely, near the Si adatoms or between adatoms, the V shapes are stretched by 0.09±0.02 nm [marked as B in Fig. 8(a)] with respect to V shapes in adatom-free regions (marked as A), where their width is equal to (0.33±0.02) nm. Due to symmetrical arrangement of Si adatoms in 5×4 unit cell, the influence on neighboring structures is the same. Similar behavior show the BP1 on

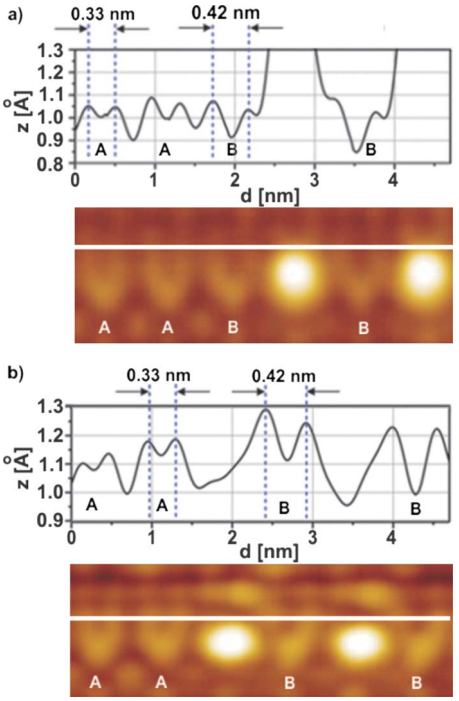

FIG. 8. (Color online) STM topography (4.7×1.7 nm^2) of (a) clean and (b) In-covered Si(111)5×2-Au surface. Panels (a) and (b) show closeup STM images presented in Figs. 1(a) and 3(a), together with corresponding cross sections along the lines shown. In both panels labels A and B stand for V shapes in BP-free region and stretched V shapes near the BP, respectively.

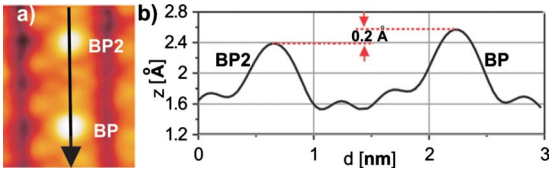

FIG. 9. (Color online) Cross section [panel (b)] of two different protrusions (BP2 and BP) on In-covered Si(111)5×2-Au surface along line shown in (a). Area of the surface shown in panel (a) is 2.4×3 nm^2. The Si adatoms (BP) appear to be 0.2 Å higher than In atoms (BP2).

Si(111)5×2-Au/In surface. The V-shape features [marked as B in panel (b) of Fig. 8] are also stretched by 0.09 nm but only inside the chains composed of bright protrusions. At the end of chains the change in V shapes depends on direction of BP1 shifts. This is another argument, which helps to identify the BP1 and BP2 protrusions on Si(111)5×2-Au/In surface.

Finally, the question arises how to distinguish In atoms located in Si-adatom sites (BP2) from Si adatoms (BP), as both kinds of protrusions show similar behavior in STM topography. It turns out that one can identify BP2 and BP features on the basis of spectroscopy, as it will be shown in Sec. VI. Moreover, the differences also exist in topography images. The Si adatoms (BP) appear to be 0.2 Å higher than In atoms (BP2) in STM topography, as shown in Fig. 9. The above criteria can help to distinguish Si adatoms from In atoms on In-covered Si(111)5×2-Au surface in unambiguous way.

VI. ELECTRONIC PROPERTIES

In order to shed some light on electronic properties of the surface structures, we have performed STS measurements. An useful quantity is normalized differential conductance $(dI/dU)/(I/U)$, which in first approximation gives local density of states (LDOS) of the surface.[46] In the following we use dI/dU which was obtained by numerical differentiating $I(U)$ characteristics.

Figure 10 shows tunneling current $I(U)$ and corresponding normalized dI/dU characteristics of different areas of Si(111)5×2-Au surface. Panel (a) shows $I(U)$ and dI/dU data taken over areas containing chains of Si adatoms [solid (blue) line] and adatom-free areas [dashed (red) line].

It is generally accepted that metallic and semiconducting character of 5×2-Au surface depends on concentration of silicon adatoms; BP-free segments are metallic while those containing Si adatoms separated by $4a_0$ are semiconducting.[8,13,24] In our experiment metallic and semiconducting character of those segments is not clear, in both cases STS spectra seem to show (0.25 ± 0.1) eV energy gap. Only the asymmetry in LDOS of the area with BP for occupied and unoccupied states is observed, and one can indicate some electronic states reported before.[13]

Deposition of 0.025 ML of Indium on Si(111)5×2-Au surface results in modifications of dI/dU characteristics, mainly in areas containing bright protrusions. This is shown in Fig. 11. As one can read off from the top panel of the figure, dI/dU point characteristics taken over BP1 and BP2

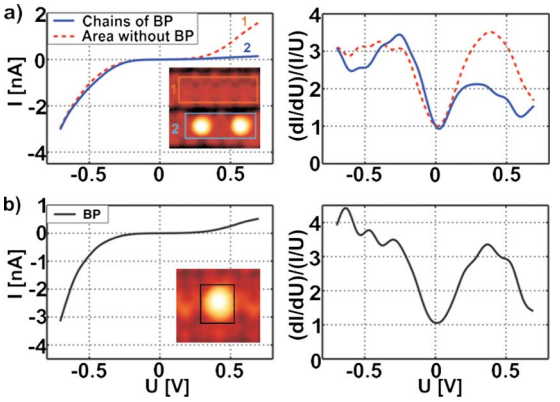

FIG. 10. (Color online) Tunneling current I (left panels) and normalized conductance $(dI/dU)/(I/U)$ (right panels) vs sample bias of different areas of Si(111)5×2-Au surface. Panel (a) shows $I(u)$ and (dI/dU) characteristics taken over an area containing a few Si adatoms [solid (blue) line] and adatom-free area [dashed (red) line], presented in the inset. Panel (b) shows point characteristics of Si adatoms. Imaging conditions during spectroscopy were $U=-0.7$ V and $I=3$ nA.

show very similar behavior. In particular, they show an electron state around 0.6–0.7 eV above the Fermi energy, associated with In atoms. On the other hand, dI/dU point characteristics taken over BP on 5×2 surface feature a state around +0.3 eV. This is additional argument that both, BP1 and BP2 features on In-induced 5×2 reconstruction, must be associated with In atoms, as the dI/dU spectra are similar to each other, and significantly differ from dI/dU spectra of BP on In-free 5×2 surface. Similar conclusions can be drawn from calculated density of states, shown in Fig. 12. To be more precise, Fig. 12 shows a comparison of projected den-

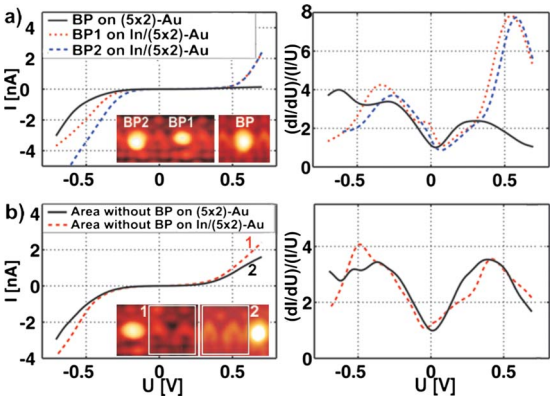

FIG. 11. (Color online) Top panel: Point characteristics $I(u)$ and normalized dI/dU of BP1 [dotted (red) lines] and BP2 [dashed (blue) lines] on Si(111)5×2-Au/In surface. For comparison, the point STS characteristics of BP [solid (black) lines] on bare Si(111)5×2-Au surface are also shown. Bottom panel: STS characteristics of the areas free of BP on bare [solid (black) lines] and on In-covered Si(111)5×2-Au surface [dashed (red) lines]. Insets represent areas of the surface where the spectroscopy was measured. Imaging conditions during spectroscopy were $U=-0.7$ V, $I=3$ nA [bare Si(111)5×2-Au surface] and $U=-0.7$ V, $I=2.5$ nA (with In deposited).

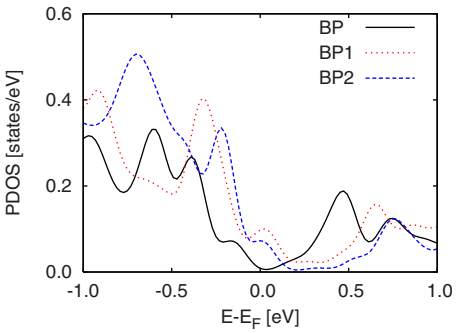

FIG. 12. (Color online) The PDOS of In and neighboring to In atoms (atoms bonded to In) on In-covered Si(111)5×2-Au surface (BP1—dotted red line and BP2—dashed blue line) together with PDOS of Si adatoms on bare Si(111)5×2-Au surface (solid black line).

sity of states (PDOS) of In and neighboring to In atoms (atoms bonded to In) with PDOS of Si adatoms on bare Si(111)5×2-Au surface. Although, the results of calculations in empty-state regime should be taken with caution, due to known limitations of the DFT theory, qualitative behavior of the density of states is the same, as in measured dI/dU characteristics. Again, the PDOS spectra of BP1 and BP2 show electron state at the energy (+0.65–0.75 eV) while PDOS of BP on bare 5×2 surface features an electron state at energy +0.45 eV. This further supports our picture on dual mechanism of In adsorption on Si(111)5×2-Au surface.

The behavior of different kinds of bright protrusions in STM topography and spectroscopy is summarized in Table II.

TABLE II. Main features of different types of bright protrusions (BP, BP1, and BP2) observed in STM topography and spectroscopy.

Type	Origin	Topography	Spectroscopy
BP	Si adatom	Visible at both polarizations	Wide resonance at E=+0.3 eV
BP1	In atom bonded to Si adatom	Visible only at positive bias	Narrow resonance at E=+0.6 eV
BP2	In atom in place of Si adatom	Visible at both polarizations (0.2 Å lower than BP)	Narrow resonance at E=+0.7 eV (similar as BP1)

VII. CONCLUSIONS

In conclusion, using scanning tunneling microscopy and spectroscopy together with first-principles DFT calculations we have studied structural and electronic properties of indium chains on Si(111)5×2-Au surface. (i) The STM topography data show that submonolayer coverage of indium leads to a well-ordered chain structure with the same periodicity as the Si adatoms form on Si(111)5×2-Au surface. (ii) We have found three kinds of bright protrusions on In-covered Si(111)5×2-Au surface, one observed in empty-state images (BP1) and the other ones (BP2 and BP) observed at both bias polarizations. With help of DFT and STS data they were interpreted as In atoms bonded to Si adatoms (BP1), In atoms located in Si-adatom sites (BP2), and Si adatoms (BP). (iii) The proposed structural model of In-induced Si(111)5×2-Au surface very well describes all the STM/STS data.

ACKNOWLEDGMENT

This work has been supported by the Polish Ministry of Education and Science under Grant No. N N202 1468 33.

*krawiec@kft.umcs.lublin.pl

[1] H. E. Bishop and J. C. Riviere, J. Phys. D **2**, 1635 (1969).
[2] H. Lipson and K. E. Singer, J. Phys. C **7**, 12 (1974).
[3] E. Bauer, Surf. Sci. Lett. **250**, L379 (1991).
[4] G. Lelay and J. P. Faurie, Surf. Sci. **69**, 295 (1977).
[5] L. E. Berman, B. W. Batterman, and J. M. Blakely, Phys. Rev. B **38**, 5397 (1988).
[6] C. Schamper, W. Moritz, H. Schulz, R. Feidenhans'l, M. Nielsen, F. Grey, and R. L. Johnson, Phys. Rev. B **43**, 12130 (1991).
[7] L. D. Marks and R. Plass, Phys. Rev. Lett. **75**, 2172 (1995).
[8] A. A. Baski, J. Nogami, and C. F. Quate, Phys. Rev. B **41**, 10247 (1990).
[9] J. D. O'Mahony, J. F. McGilp, C. F. J. Flipse, P. Weightman, and F. M. Leibsle, Phys. Rev. B **49**, 2527 (1994).
[10] T. Hasegawa, S. Hosaka, and S. Hosoki, Surf. Sci. **357–358**, 858 (1996).
[11] A. Kirakosian, J. N. Crain, J.-L. Lin, J. L. McChesney, D. Y. Petrovykh, F. J. Himpsel, and R. Benewitz, Surf. Sci. **532-535**, 928 (2003).
[12] A. Kirakosian, R. Bennewitz, F. J. Himpsel, and L. W. Bruch, Phys. Rev. B **67**, 205412 (2003).
[13] H. S. Yoon, J. E. Lee, S. J. Park, I. W. Lyo, and M. H. Kang, Phys. Rev. B **72**, 155443 (2005).
[14] W. H. Choi, P. G. Kang, K. D. Ryang, and H. W. Yeom, Phys. Rev. Lett. **100**, 126801 (2008).
[15] P.-G. Kang, H. Jeong, and H. W. Yeom, Phys. Rev. Lett. **100**, 146103 (2008).
[16] I. R. Collins, J. T. Morgan, P. T. Andrews, R. Cosso, and J. D. O'Mahony, Surf. Sci. **325**, 45 (1995).
[17] K. N. Altmann, J. N. Crain, A. Kirakosian, J. L. Lin, D. Y. Petrovykh, F. J. Himpsel, and R. Losio, Phys. Rev. B **64**, 035406 (2001).
[18] R. Losio, K. N. Altmann, and F. J. Himpsel, Phys. Rev. Lett. **85**, 808 (2000).
[19] I. Matsuda, M. Hengsberger, F. Baumberger, T. Greber, H. W. Yeom, and J. Osterwalder, Phys. Rev. B **68**, 195319 (2003).
[20] J. L. McChesney, J. N. Crain, V. Perez-Dieste, F. Zheng, M. C.

Gallagher, M. Bissen, C. Gundelach, and F. J. Himpsel, Phys. Rev. B **70**, 195430 (2004).
[21] I. G. Hill and A. B. McLean, Phys. Rev. B **55**, 15664 (1997).
[22] M.-H. Kang and J. Y. Lee, Surf. Sci. **531**, 1 (2003).
[23] S. C. Erwin, Phys. Rev. Lett. **91**, 206101 (2003).
[24] S. Riikonen and D. Sanchez-Portal, Phys. Rev. B **71**, 235423 (2005).
[25] C.-Y. Ren, S.-F. Tsay, and F.-C. Chuang, Phys. Rev. B **76**, 075414 (2007).
[26] F.-C. Chuang, C.-H. Hsu, C.-Z. Wang, and K.-M. Ho, Phys. Rev. B **77**, 153409 (2008).
[27] J. D. O'Mahony, C. H. Patterson, J. F. McGilp, F. M. Leibsle, P. Weightman, and C. F. J. Flipse, Surf. Sci. Lett. **277**, L57 (1992).
[28] S. C. Erwin and H. H. Weitering, Phys. Rev. Lett. **81**, 2296 (1998).
[29] M. H. Kang, J. H. Kang, and S. Jeong, Phys. Rev. B **58**, R13359 (1998).
[30] J. N. Crain, J. L. McChesney, F. Zheng, M. C. Gallagher, P. C. Snijders, M. Bissen, C. Gundelach, S. C. Erwin, and F. J. Himpsel, Phys. Rev. B **69**, 125401 (2004).
[31] J. Nogami, S. I. Park, and C. F. Quate, Phys. Rev. B **36**, 6221 (1987).
[32] J. Kraft, M. G. Ramsey, and F. P. Netzer, Phys. Rev. B **55**, 5384 (1997).
[33] K. Skrobas, R. Zdyb, M. Kisiel, and M. Jałochowski, Mater. Sci. (Poland) **26**, 55 (2008).
[34] J. R. Ahn, P.-G. Kang, J. H. Byun, and H. W. Yeom, Phys. Rev. B **77**, 035401 (2008).
[35] P.-G. Kang, H. Jeong, and H. W. Yeom, Phys. Rev. B **79**, 113403 (2009).
[36] C. Gonzalez, J. Guo, J. Ortega, F. Flores, and H. H. Weitering, Phys. Rev. Lett. **102**, 115501 (2009).
[37] P. Ordejon, E. Artacho, and J. M. Soler, Phys. Rev. B **53**, R10441 (1996).
[38] D. Sanchez-Portal, P. Ordejon, E. Artacho, and J. M. Soler, Int. J. Quantum Chem. **65**, 453 (1997).
[39] E. Artacho, D. Sanchez-Portal, P. Ordejon, A. Garcia, and J. M. Soler, Phys. Status Solidi B **215**, 809 (1999).
[40] J. M. Soler, E. Artacho, J. D. Gale, A. Garcia, J. Junquera, P. Ordejon, and D. Sanchez-Portal, J. Phys.: Condens. Matter **14**, 2745 (2002).
[41] E. Artacho, E. Anglada, O. Dieguez, J. D. Gale, A. Garcia, J. Junquera, R. M. Martin, P. Ordejon, J. M. Pruneda, D. Sanchez-Portal, and J. M. Soler, J. Phys.: Condens. Matter **20**, 064208 (2008).
[42] J. P. Perdew and A. Zunger, Phys. Rev. B **23**, 5048 (1981).
[43] N. Troullier and J. L. Martins, Phys. Rev. B **43**, 1993 (1991).
[44] M. Yoon and R. F. Willis, Surf. Sci. **512**, 255 (2002).
[45] M. Saito, H. Sasaki, M. Mori, T. Tambo, and C. Tatsuyama, e-J. Surf. Sci. Nanotechnol. **3**, 244 (2005).
[46] M. Passoni, F. Donati, A. Li Bassi, C. S. Casari, and C. E. Bottani, Phys. Rev. B **79**, 045404 (2009).